# Modeling and Practical Design Dual-Mode Sinewave and Common Mode Filter for PWM Motor Drives System Using Tricore Laminations

Tin Luu
Senior Product Engineer
MTE Corporation
Menomonee Falls WI, USA
Tin.luu@mtecorp.com

***Abstract*—A dual-mode sinewave output filter that eliminates motor problems due to the PWM waveforms in both common mode and differential mode operation is proposed. A three-phase inductor constructed with tricore laminations. The windings possess differential mode inductance and proportionally every large common mode inductance characteristic. In voltage source converters, the common mode voltage is mainly distributed in the switching frequency range, therefore the common mode voltage in this filter design is in the medium frequency range referring to the switching frequency and sidebands of its integral multiples. The single integrated inductor with the capacitors creates a LC low-pass filter in both common mode and differential mode operation. This proposed filter offers a complete solution with reliable, practical and cost-effective to the issues caused by common mode voltage in power converter systems. Three different rating of 5A, 45A and 160A prototypes were built, and test results presented.**

***Keywords— Common mode (CM); differential mode (DM); PWM; tricore laminations***

## I. INTRODUCTION

PWM (Pulse-width modulated) inverter systems have been widely used throughout the industries. They are used on variable-speed drives to power motors. Common mode voltage (CMV) is generated by the switching action of solid-state devices in power converters. There have been challenges to reduce the negative effects of the common mode voltage that these inverter systems produce. At the most catastrophic level, ringing of the common mode voltages and currents can cause premature failure of the motor bearings, motor windings, and cables [1]. The CMV is not only damage the insulation system in the motor drives [2-4], but also induced shaft voltage, ground leakage and bearing currents. The shaft voltage and bearing currents are the reason for bearing failure [5-8]. Applications with lead lengths under 305 meters can benefit from *dV/dt* filter that includes both DM and CM impedance with damping matched to the cable surge impedance. These filters reduced reflection of both DM and CM traveling waves [9-10]. Alternate filter solutions to essentially eliminate PWM CM and DM harmonics have been proposed [11-12]. These options either have multiple filter sections that address the CM and DM filtering separately or using a complex control of multi-phase power technique by adding extra legs to the conventional two-level inverter. This paper proposes an integrated filter solution that includes both DM and CM filtering. This paper will present the magnetic design and filtering solution. Experimental filters of 5A, 45A and 160A in a 480V system based on the proposed solution are built and tested with motor application.

## II. ANALYSIS OF CM VOLTAGE IN VOLTAGE SOURCE CONVERTERS

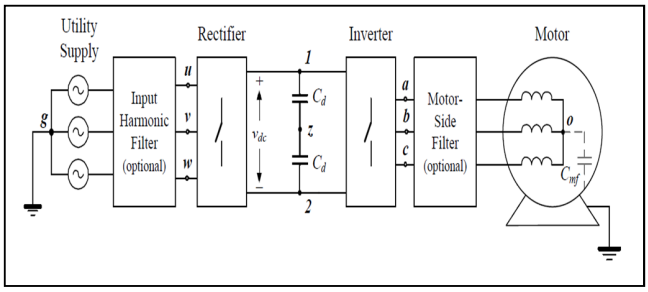


Fig. 1. Voltage source inverter diagram

Fig. 1 shows a simplified of voltage source inverter diagram. The CM voltage of the rectifier and inverter in a balanced three-phase system can be written as

$$V_{CM-REC} = -\frac{V_{uz} + V_{vz} + V_{wz}}{3} \quad (1)$$

$$V_{CM-INV} = \frac{V_{az} + V_{bz} + V_{cz}}{3} \quad (2)$$

$V_{uz}$, $V_{vz}$ and $V_{wz}$ are the rectifier AC voltages to the DC-link midpoint and $V_{az}$, $V_{bz}$ and $V_{cz}$ are the inverter output voltages to the DC-link midpoint. The total common mode voltage of the system is calculated as

$$V_{CM-TOTAL} = V_{CM-INV} + V_{CM-REC}$$

$$= \frac{V_{az} + V_{bz} + V_{cz}}{3} - \frac{V_{uz} + V_{vz} + V_{wz}}{3} \quad (3)$$

For two-level of voltage source converter, the CM voltage can be calculated by the switching functions:

$$V_{CM-INV} = \frac{V_{az} + V_{bz} + V_{cz}}{3}$$
$$= \frac{V_{dc}}{3}(S_a + S_b + S_c) - \frac{V_{dc}}{2} \quad (4)$$

$S_a$, $S_b$ and $S_c$ are the switching function of phase a, b and c. The common mode voltage is determined by the switching functions with the values of $\pm\frac{V_{dc}}{6}$ and $\pm\frac{V_{dc}}{2}$. The total common mode voltage is calculated from the rectifier and inverter. It depends on the converter topologies, modulation techniques and operating condition of the drive [13-15]. The common mode voltage produced by the diode bridge rectifier and PWM inverter are distributed separately at the triple line frequency (180Hz) and the carrier frequency as well as the sidebands of its integer multipliers. The CMV magnitudes of the diode bridge rectifier are determined by three-phase AC voltages and the CMV components at the triple fundamental frequency dominate the spectra. The CMV in voltage source converters are stepwise waveforms with fractional values of the DC voltage.

## III. THEORETICAL ANALYSIS OF PROPOSED FILTER

If the CMV are not mitigated in a motor drive, they will appear on the neutral point of the stator windings with respect to the ground. The motor line-to-ground voltage will be increased significantly and that leading to premature failure of the motor winding insulations systems and caused the life of the motor reduced[16-17]. Proposed filter circuit is shown in Fig. 2. Capacitors DM CAP (differential mode capacitors) are solely for differential mode filtering. Capacitors CM CAP (common mode capacitors) are for common mode filtering. Each phase will have two common mode capacitors connected to DC+ and DC- of the DC bus. The common mode currents travelling from the VFD through the cable to the motor and to the parasitic capacitors and return to the VFD.

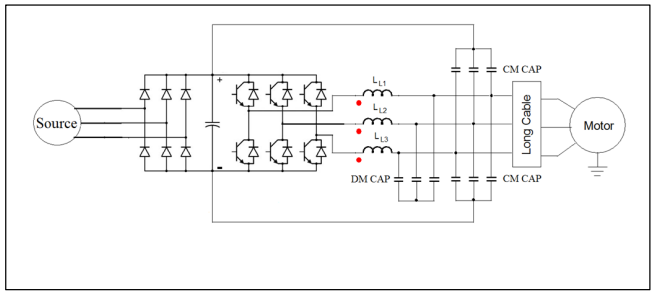


Fig. 2. Filter topology

For DM filtering, assuming there is some resistance R that account for the internal resistance of the inductor and it is very small. From Fig. 2, resistor R, $L_{L1}$ and DM capacitor of phase A are formed a second order low-pass filter. The voltage gain for a single phase low-pass filter can be written as

$$\frac{V_{out}}{V_{in}} = \frac{1}{LCs^2 + RCs + 1} \quad (5)$$

The frequency domain analysis for this typical low-pass filter is

$$H(s) = \frac{\omega^2}{s^2 + \frac{\omega}{Q}s + \omega^2} \quad (6)$$

Where s =jω, ω is the natural oscillating frequency and Q is the quality factor. When H(s) is maximum $Q>1/\sqrt{2}$. Rearrange (6) and comparing the coefficients with (5)

$$LC = \frac{1}{\omega^2} \quad (7)$$

$$RC = \frac{1}{Q\omega} \quad (8)$$

The simple guideline to design LC low-pass filter for the inverter as follow

1) Know the carrier frequency of PWM and the fundamental frequency
2) Do not want to raise the output impedance of the inverter by large amount
3) Design inductors that carry the rated current of the inverter without overheating, having excessive voltage drop or saturating
4) Need capacitors that are rated for the ripple current they will be carrying

In general, if the system voltage is V (Volt line to line RMS), the inverter rating current is A (Amp RMS), this inverter will have a load impedance of Z=V/A (OHM) at full load. Assume the PWM switching frequency = Fsw (Hz) and fundamental frequency = f (Hz). The resonant frequency is chosen base on the switching frequency Fsw. If Fsw is less than or equal to 2000 Hz, the resonant frequency can be chosen from the range of 25% to 35% of the switching frequency. After the load impedance Z and resonant frequency are chosen, the parameters of the filter can be estimated

$$L_{Filter} = \frac{Z}{2\pi F_{resonance}} \quad (9)$$

$$C_{Filter} = \frac{1}{2\pi F_{resonance} Z} \quad (10)$$

Now re-calculate the impedance of the components of the filter at fundamental frequency and switching frequency. Assume this impedance is $Z_{RECAL}$ (ohm). The circulating current at fundamental frequency can be calculated as

$$I_{Circulating} = \frac{V(system\ voltage)}{Z_{RECAL}} \quad (11)$$

The design engineer could shift the filter frequency upward to minimize the circulating current, component size and cost. The resonance frequency of common mode filter will be tuned the same as the differential mode filter. In this case the design engineer just needs to find the value of common mode capacitance since the common mode inductance has already known from the design of the inductor.

## IV. MAGNETIC DESIGN AND ANALYSIS OF THREE-PHASE TRICORE INDUCTOR

In these designs, the system voltage is 480V. Filters are 5A, 45A and 160A. Fundamental frequency is 60Hz. Percent impedance of the inductance is around 8% to 10%. Maxwell magnetic design and analysis are shown in Fig. 3 and Fig. 4.

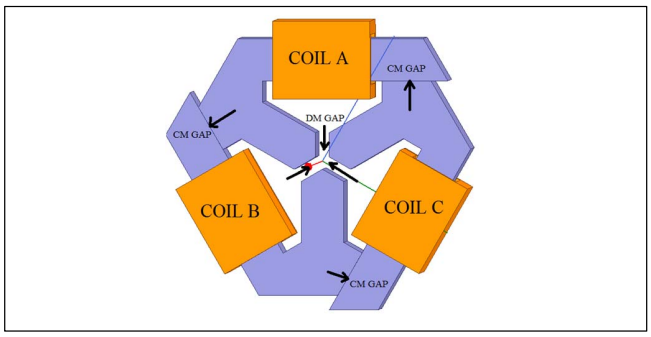


Fig. 3. Hexagonal construction

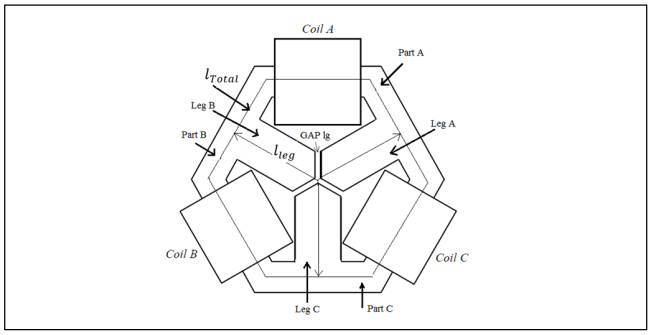


Fig. 4. Integrated inductor analysis

Fig. 4 shows the integrated magnetic core of hexagonal construction. $i_A$, $i_B$, $i_C$ are three-phase currents of both DM and CM. $Ni_A$, $Ni_B$, $Ni_C$ are the magnetomotive forces (MMF), N is the number of turns of the Coil A, Coil B and Coil C. $\Re_{Total}$ is the total reluctance of the hexagonal core. The reluctances of part A, ($\Re_{pA}$), part B ($\Re_{pB}$), and part C ($\Re_{pC}$) is one-third of the total core due to the symmetrical of the construction.

$$\Re_{pA} = \Re_{pB} = \Re_{pC} = \frac{\Re_{Total}}{3} = \frac{l_{Total}}{3\mu_0\mu_r A_c} \tag{12}$$

$l_{Total}$ and $A_c$ are the perimeter and cross-sectional area of the hexagonal core. $\mu_0$ and $\mu_r$ are the permeability of air and relative permeability of the core material. $l_{leg}$ and $A_b$ are the length and cross-sectional area of the leg. The reluctances of Leg A, Leg B and Leg C are

$$\Re_{legA} = \Re_{legB} = \Re_{legC} = \Re_{Leg} = \frac{l_{leg}}{\mu_0\mu_r A_b} \tag{13}$$

The reluctances of the gaps are calculated as

$$\Re_{gapA} = \Re_{gapB} = \Re_{gapC} = \Re_{gap} = \frac{l_g}{\mu_0\left(\frac{A_b}{\sqrt{3}}\right)} \tag{14}$$

Let called $\Re_{EQU} = \frac{\Re_{Total}}{3} + 2\Re_{Leg} + \Re_{gap}$ the reluctance, MMF and flux matrixes are

$$\Re = \begin{bmatrix} \Re_{EQU} & -\Re_{Leg} & -\Re_{Leg} & -\Re_{gap} \\ -\Re_{Leg} & \Re_{EQU} & -\Re_{Leg} & -\Re_{gap} \\ -\Re_{Leg} & -\Re_{Leg} & \Re_{EQU} & -\Re_{gap} \\ -\Re_{gap} & -\Re_{gap} & -\Re_{gap} & -3\Re_{gap} \end{bmatrix} \tag{15}$$

$$F = (Ni_A \quad Ni_B \quad Ni_C \quad 0)^T \tag{16}$$

$$\Phi = (\Phi_A \quad \Phi_B \quad \Phi_C \quad \Phi_{gap})^T \tag{17}$$

The flux matrix is calculated by using the following equation

$$\Re \cdot \Phi = F \tag{18}$$

The Flux $\Phi_A, \Phi_B, \Phi_C$ are one-third of total flux that represent the flux of Part A, Part B and Part C. To simplify the equation let called

$$D = \frac{\Re_{Total}}{3}\left(\frac{\Re_{Total}}{3} + 3\Re_{Leg} + \Re_{gap}\right) \tag{19}$$

$$\Re_A = \frac{\Re_{Total}}{3} + \Re_{Leg} + \frac{\Re_{gap}}{3} \tag{20}$$

$$\Re_B = \Re_{Leg} + \frac{\Re_{gap}}{3} \tag{21}$$

$$\begin{bmatrix} \Phi_A \\ \Phi_B \\ \Phi_C \\ \Phi_{gap} \end{bmatrix} = \begin{bmatrix} \frac{Ni_A\Re_A}{D} + \frac{Ni_B\Re_B}{D} + \frac{Ni_C\Re_B}{D} \\ \frac{Ni_A\Re_B}{D} + \frac{Ni_B\Re_A}{D} + \frac{Ni_C\Re_B}{D} \\ \frac{Ni_A\Re_B}{D} + \frac{Ni_B\Re_B}{D} + \frac{Ni_C\Re_A}{D} \\ \frac{Ni_A}{\Re_{Total}} + \frac{Ni_B}{\Re_{Total}} + \frac{Ni_C}{\Re_{Total}} \end{bmatrix} \tag{22}$$

The flux of the legs and air gap can be calculated as

$$\Phi_{legA} = \Phi_A - \Phi_B = \frac{N(i_A - i_B)}{\frac{\Re_{Total}}{3} + 3\Re_{Leg} + \Re_{gap}} \tag{23}$$

$$\Phi_{legB} = \Phi_B - \Phi_C = \frac{N(i_B - i_C)}{\frac{\Re_{Total}}{3} + 3\Re_{Leg} + \Re_{gap}} \tag{24}$$

$$\Phi_{legC} = \Phi_C - \Phi_A = \frac{N(i_C - i_A)}{\frac{\Re_{Total}}{3} + 3\Re_{Leg} + \Re_{gap}} \tag{25}$$

$$\Phi_{gapA} = \Phi_A - \Phi_{gap} \tag{26}$$

$$\Phi_{gapB} = \Phi_B - \Phi_{gap} \tag{27}$$

$$\Phi_{gapC} = \Phi_C - \Phi_{gap} \tag{28}$$

Assuming three-phase DM currents are balance and $i_{DM\,A} + i_{DM\,B} + i_{DM\,C} = 0$. The differential mode flux of Part A, Part B, Part C, Leg A, Leg B, and Leg C also calculated as

$$\Phi_{DM\,Part\,A} = \Phi_{DM\,gap\,A} = \frac{Ni_{DM\,A}}{\frac{\Re_{Total}}{3} + 3\Re_{Leg} + \Re_{gap}} \tag{29}$$

$$\Phi_{DM\ Part\ B} = \Phi_{DM\ gap\ B} = \frac{Ni_{DM\ B}}{\frac{\Re_{Total}}{3} + 3\Re_{Leg} + \Re_{gap}} \quad (30)$$

$$\Phi_{DM\ Part\ C} = \Phi_{DM\ gap\ C} = \frac{Ni_{DM\ C}}{\frac{\Re_{Total}}{3} + 3\Re_{Leg} + \Re_{gap}} \quad (31)$$

$$\Phi_{DM\ Leg\ A} = \frac{N(i_{DM\ A} - i_{DM\ B})}{\frac{\Re_{Total}}{3} + 3\Re_{Leg} + \Re_{gap}} \quad (32)$$

$$\Phi_{DM\ Leg\ B} = \frac{N(i_{DM\ B} - i_{DM\ C})}{\frac{\Re_{Total}}{3} + 3\Re_{Leg} + \Re_{gap}} \quad (33)$$

$$\Phi_{DM\ Leg\ C} = \frac{N(i_{DM\ C} - i_{DM\ A})}{\frac{\Re_{Total}}{3} + 3\Re_{Leg} + \Re_{gap}} \quad (34)$$

The DM inductance each phase can be calculated as

$$L_{DM} = \frac{N\Phi_{DM\ Total}}{i_{DM}} = \frac{N^2}{\frac{\Re_{Total}}{3} + 3\Re_{Leg} + \Re_{gap}} \quad (35)$$

For CM inductance calculation, the CM current each phase is one-third of the total CM current.

$$i_{CM\ A} = i_{CM\ B} = i_{CM\ C} = \frac{i_{CM\ Total}}{3} \quad (36)$$

$$\Phi_{CM\ Part\ A} = \Phi_{CM\ Part\ B} = \Phi_{CM\ Part\ C} = \Phi_{CM} = \frac{Ni_{CM\ Total}}{\Re_{Total}} \quad (37)$$

$$\Phi_{CM\ Leg\ A} = \Phi_{CM\ Leg\ B} = \Phi_{CM\ Leg\ C} = 0 \quad (38)$$

$$\Phi_{CM\ gap\ A} = \Phi_{CM\ gap\ B} = \Phi_{CM\ gap\ C} = 0 \quad (39)$$

The common mode inductance of each phase is

$$L_{CM\ phase\ A} = L_{CM\ phase\ B} = L_{CM\ phase\ C} = \frac{N\Phi_{CM}}{\frac{i_{CM}}{3}} = \frac{3N^2}{\Re_{Total}} \quad (40)$$

The total common inductance is

$$L_{CM\ Total} = \frac{L_{CM\ phase\ A}}{3} = \frac{N^2}{\Re_{Total}} \quad (41)$$

Another method for estimate calculating the common mode inductance is using Maxwell.

$$L_{CM} = \frac{1}{\frac{1}{L_A + M_{AB} + M_{AC}} + \frac{1}{L_B + M_{BC} + M_{BA}} + \frac{1}{L_C + M_{CA} + M_{CB}}} \quad (42)$$

$L_A$, $L_B$, and $L_C$ are multiple turns inductance of phase A, B and C. $M_{AB}$, $M_{BA}$, $M_{AC}$, $M_{CA}$, $M_{BC}$ and $M_{CB}$ are mutual inductances. The common mode inductance is measured by connecting all the starts of three-phase coils together and all the finishes of three-phase coils together then apply voltage to these two new terminals and measuring the current that shows in Fig. 5. Common mode gap is required to be minimal to maximize the common mode inductance. Common mode gap and differential gap are shown in Fig. 6.

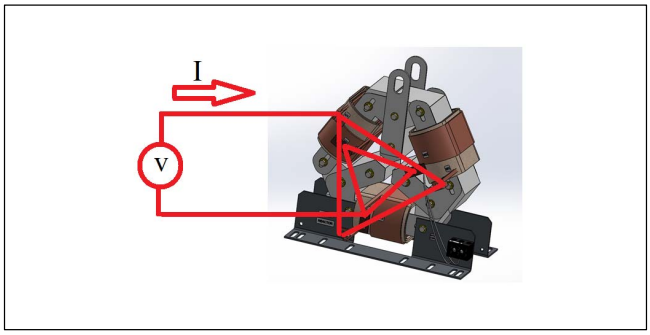


Fig. 5. CM inductance test

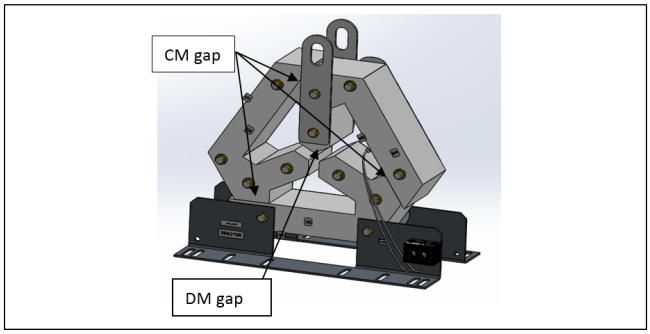


Fig. 6. CM and DM gap

## V. SIMULATION RESULTS

These design filters are sinewave output filters with the common mode characteristic. The example filters are designed with 480V system, 60Hz fundamental frequency, 4kHz switching frequency, 5A, 45A, 160A ratings with 3HP, 30HP and 125HP VFD and motor system. Table I shows the 45A filter design parameters.

TABLE I. FILTER DESIGN PARAMETERS FOR 45A

| | | |
|---|---|---|
| $L_{DM}$ | Input inductance | 1.48 mH |
| $L_{CM}$ | CM inductance | 32.5 mH |
| $C_{DM}$ | DM capacitance | 38.8 µF |
| $C_{CM}$ | CM capacitance | 2.0 µF |

Fig. 7-10 show DM simulation results of the inverter voltage (516V rms), motor voltage (458V rms), inverter current (45A rms) and motor current (45A rms). THVD of motor voltage is 2.3%. Fig. 11-12 show simulation results of the CM inverter voltage (128V rms, 650V peak-peak), CM motor voltage (46V rms, 140.0V peak-peak). Fig. 13-14 show the simulation results of total CM capacitor current (0.38A rms) and line-to-ground voltage at the motor (269V rms). Fig. 15-16 show the FFT of inverter and motor CM voltage. Simulation results show the DM and CM voltage both without and with the filter respectively. THVD of the motor voltage is around 3.0% and

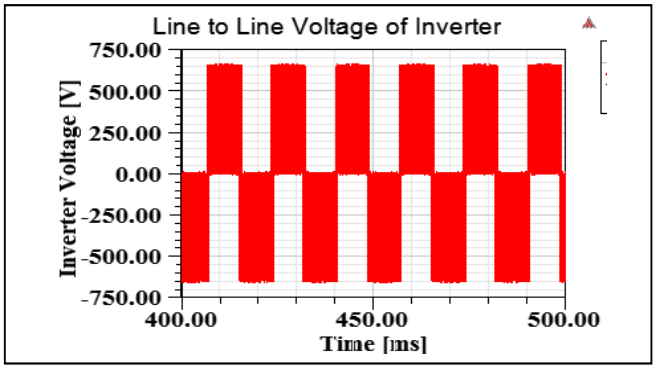


Fig. 7. DM inverter voltage

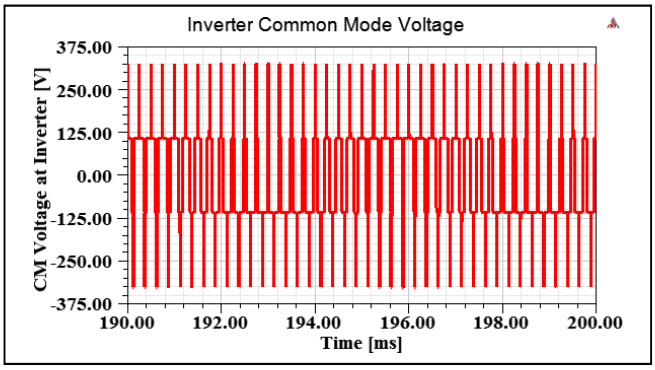


Fig. 11. CM voltage at inverter

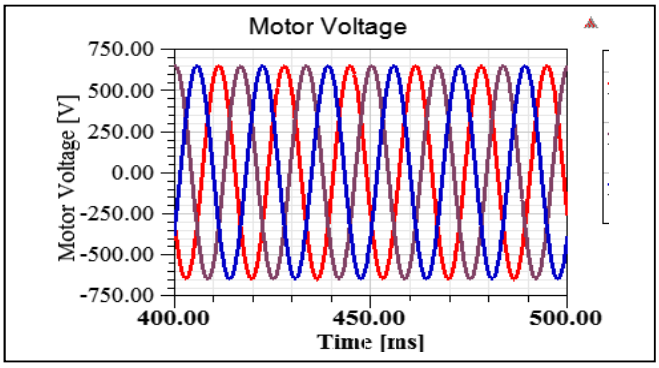


Fig. 8. DM motor voltage

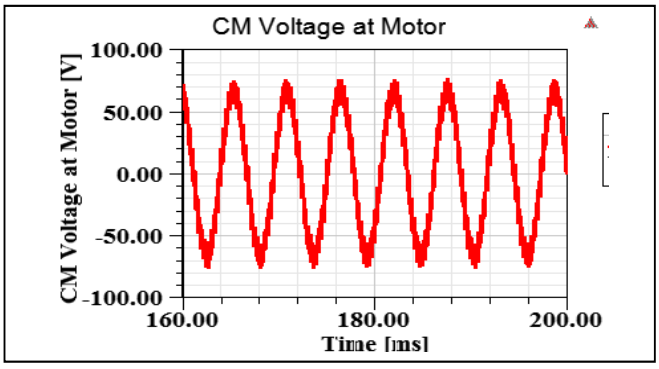


Fig. 12. CM voltage at the motor

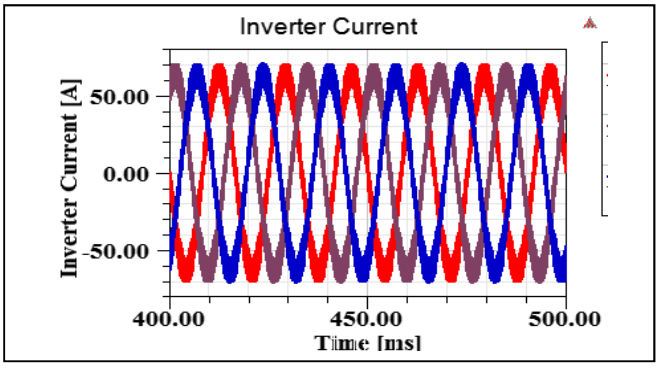


Fig. 9. DM inverter current

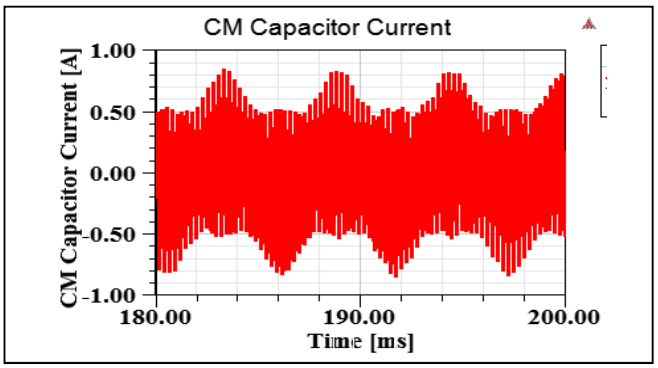


Fig. 13. CM capacitor current

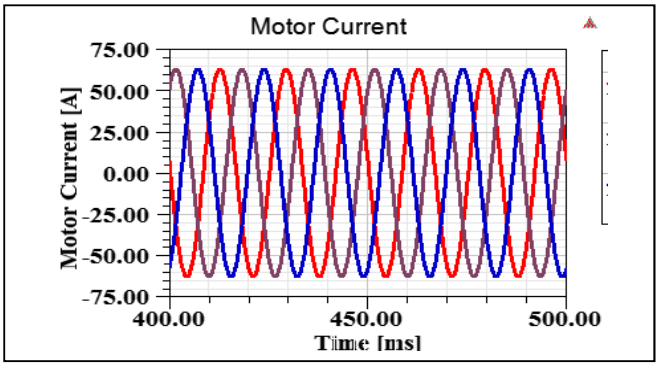


Fig. 10. DM Motor current

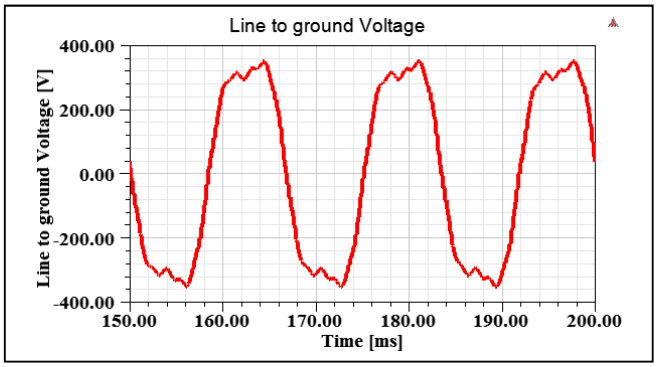


Fig. 14. Line-to-ground voltage at the motor

the peak common mode voltage reduces up to 90%. Common mode filter can reduce the common mode peak voltage and remove all high amplitudes of harmonics frequency around switching frequency and sidebands of its integral multiples. Common mode filter did not remove the low frequency such as third harmonics and sideband of its integral multiples.

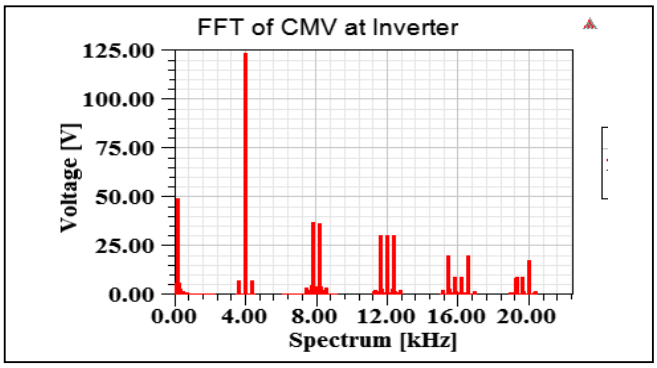


Fig. 15. FFT of CM voltage at inverter

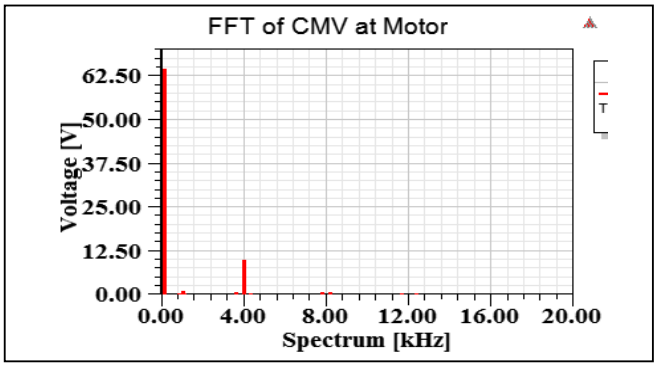


Fig. 16. FFT CM voltage at the motor

## VI. EXPERIMENTAL RESULTS

The experimental setup was built in the laboratory of MTE Corporation consisting of a 480V 60Hz three-phase power supply, a commercial 5A, 45A, 160A rating filters with 3HP, 30HP and 125HP VFD and motors system. The prototype is in Fig. 17 and filter's paramters for 45A are shown in Table. 1. Fig. 18-23 demonstrate the results of 45A filter at 5kHz switching frequency. Fig. 18 shows DM inverter voltage (492.8V rms), DM inverter current (43.51A rms), DM motor voltage (440.7V rms), DM motor current (45.35A rms) at full load. Fig. 19 shows CM inverter voltage (114.2V rms), CM inverter current (2.13A rms), CM motor voltage (48.4V rms), CM motor current (0.688A rms). Fig. 20 shows the CM currents before and after using 45A filter. Fig. 21 shows the shaft voltage (Yellow 0.646V rms) and CM voltage at the motor (Blue 109.58V rms). Fig. 22-23 show the FFT of the CM voltage at the inverter and at the motor. The summary of the completed laboratory test results is shown in Table. II.

TABLE II. LABORATORY TEST RESULTS

| Amps | HP | Part Number | Temp Rise (°C) | Common Mode Attenuation (dB) | Common Mode Attenuation (%) | THVD (%) | Efficiency (%) | Insertion Loss (%) | Sound Level (dBA) |
|---|---|---|---|---|---|---|---|---|---|
| Specification Targets | | | < 130C | -30dB | > 96% | 5% maximum | > 98% | 10% max @60 Hz | 75 dBA @1 meter |
| 5 | 3 | SWNx0005D | 40.00 | 21.80 | 92% | 4.50% | 99% | 9.8% | 70.00 |
| 45 | 30 | SWNx0045D | 104.00 | 24.40 | 94% | 3.40% | 98% | 9.8% | 72.00 |
| 160 | 125 | SWNx0160D | 125.00 | 22.60 | 91% | 2.30% | 99% | 10% | 74.00 |

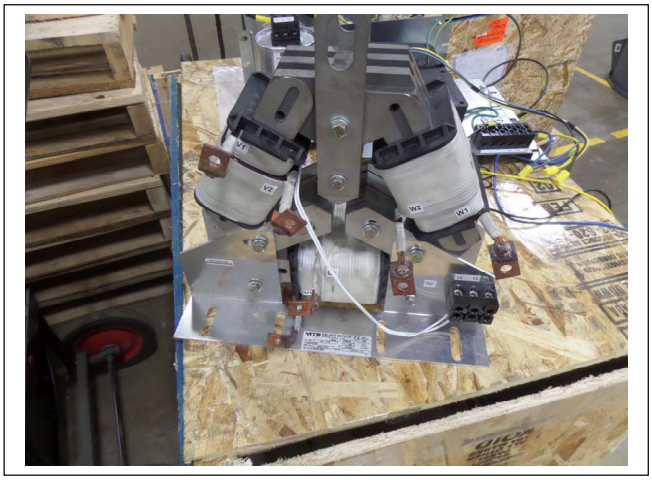

Fig. 17. Experimental of 45A filter

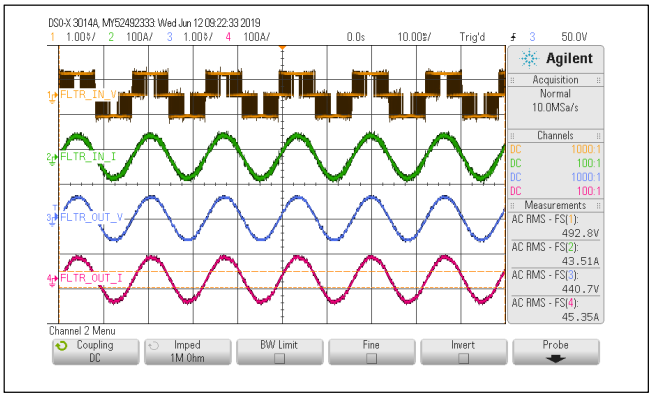


Fig. 18. DM Voltage & Current of 45A Filter

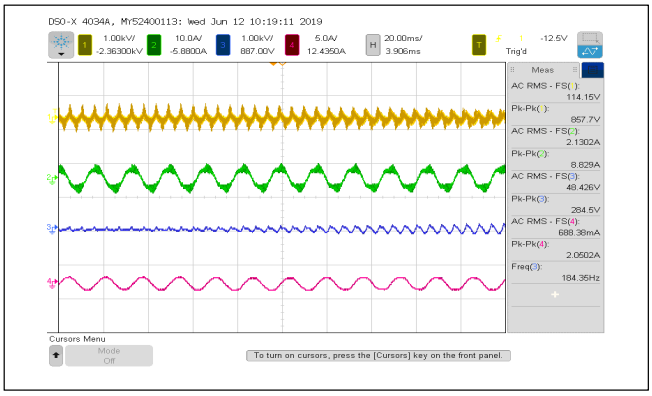


Fig. 19. CM Voltage & Current of 45A Filter

Fig. 20. CM Currents before and after using 45A filter

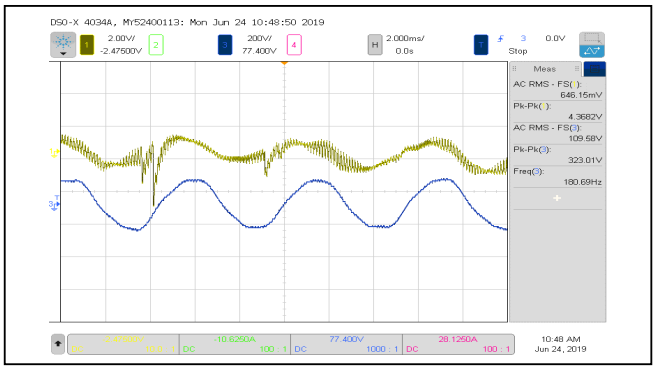

Fig. 21. Shaft Voltage & CM Voltage at the motor

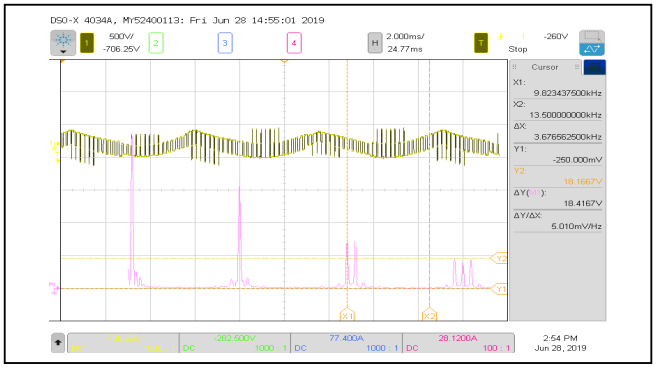

Fig. 22. FFT of CM Voltage at Inverter

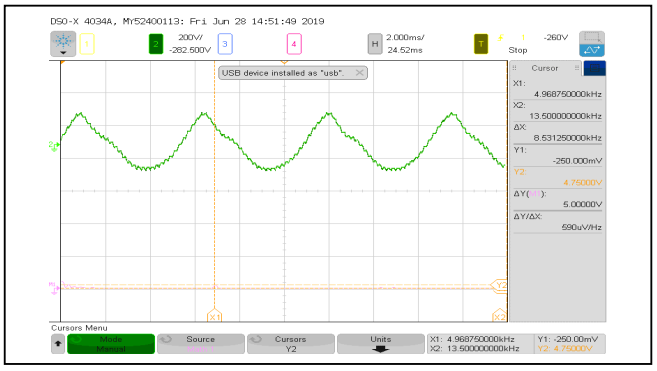

Fig. 23. FFT of CM Voltage at the motor

## VII. CONCLUSION

In this paper, the modeling and practical design dual mode sinewave and common mode filter for 480V PWM motor drives system using tricore laminations are presented. Through analysis, simulation and experimental results of the prototypes have shown that the proposed filter can reduce the differential mode THVD to less than 5%. It is also proven to reduce the common mode high frequency harmonics voltage by more than 90% especially around switching frequency and the sidebands of its integral multiples. The results also show more than 95% reduction in bearing discharges when measuring with SKF meter. The future work in this project is to test the performance of these filters with different VFD manufactures, ratings, voltage system, motor manufactures and the length of the cable up to 1000 ft or more. The results of these filters performances will help design engineers to come up with the complete solutions for this problem.

## REFERENCES


[1] T.A. Shudarek, "Understanding Adjustable Speed Drive Common Mode Problems and Effective Filter Solutions", MTE Corporation, 2015.

[2] J. Rodriguez, L. Moran, J. Pontt, R. Osorio, and S. Kouro, "Modeling and Analysis of common mode voltage generated in medium voltage PWM-CSI drives," *IEEE Trans. Power Electron.*, vol. 18, no. 3, pp. 873-879, May 2003.

[3] B. Wu and F.A. DeWinter, "Voltage stress on induction motors in medium-voltage (2300-6900V) PWM GTO CSI drives," *IEEE Trans. Power Electron.*, vol. 12, no. 2, pp. 213-220, March 1997.

[4] F. Wang, "Motor shaft voltages and bearing currents and their reduction in multilevel medium voltage PWM voltage-source-inverter drive applications," *IEEE Trans. Ind. Appl.*, vol. 36, no. 5, pp. 1336-1341, Sept./Oct., 2000.

[5] S. Chen, T.A. Lipo, and D. Fitzgerald, "Source of induction motor bearing currents caused by PWM inverters," *IEEE Trans. Energy Convers.*, vol. 11, no. 1, pp. 25-32, Mar., 1996.

[6] S. Chen and T.A. Lipo, "Circulating type motor bearing current in inverter drives," *IEEE Mag. Ind. Appl.*, vol. 4, no. 1, pp. 32-38, Jan./Feb., 1998.

[7] J.M. Erdman, R.J. Kerkman, D.W. Schlegel, and G.L. Skibinski, "Effect of PWM inverters on AC motor bearing currents and shaft voltages," *IEEE Trans. Ind. Appl.*, vol. 32, no. 1, pp-250-259, Mar./Apr., 1996.

[8] S. Chen, T.A. Lipo, and D. Fitzgerald, "Modeling of motor bearing currents in PWM inverter drives," *IEEE Trans. Ind. Appl.*, vol. 32, no. 6, pp. 1365-1370, Nov./Dec., 1996.

[9] R.M. Tallam, G.L. Skibinski, T.A. Shudarek and R.A. Lukaszewski, "Integrated Differential-Mode and Common-Mode Filter to Mitigate the Effects of Long Motor Leads on AC Drives." 2010 *IEEE Energy Conversion Congress and Exposition*, Atlanta, GA, 2010, pp.838-845.

[10] MTE Corporation. http://www.mtecorp.com/Dv-Sentry/. 2016. Print.

[11] A.L. Julian, T.A. Lipo, and D.M Divan, "Method and apparatus for reducing common mode voltage in multi-phase power converters," U.S. Patent 5852558, December 22, 1998.

[12] X. Chen, D. Xu, "A Novel Inverter-Output Passive Filter for Reducing Both Differential and Common Mode *dv/dt* at the Motor Terminals in PWM Drive Systems," *IEEE Trans. Ind, Electron.*, vol. 54, no. 1, pp-419-425, Feb. 2007.

[13] H.D. Lee and S.K. Sul, "Common mode voltage reduction in boost rectifier/inverter system by shifting active voltage vector in a control period," *IEEE Trans. Power Electron.*, vol. 15, no. 6, pp-1094-1101, Nov., 2000.

[14] H.D. Lee and S.K. Sul, "A common mode voltage reduction method modifying the distribution of zero-voltage vector in PWM

converter/inverter system," *IEEE Trans. Ind. Appl*., vol. 37, no. 6, pp-1732-1738, Nov./Dec., 2001.

[15] R.M. Tallam, R.J. Kerkman, D. Leggate and R.A. Lukaszewski, "Common mode voltage reduction PWM algorithm for AC drives," *IEEE Trans. Ind. Appl*., vol. 46, no. 5, pp. 1959-1969, Sept./Oct., 2010.

[16] B. Wu, *High-Power Converters and AC Drives*. New York/Piscataway: Wiley-IEEE Press, 2006.

[17] D.A. Rendusara, E. Cengelci, P.N. Enjeti, V.R. Stefanovic, and J.W. Gray, "Analysis of common mode voltage-"neutral shift" in medium voltage PWM adjustable speed drive (MV-ASD) systems," IEEE Trans. Power. Electron., vol. 15, no. 6. pp. 1124-1133, Nov. 2000.